Photoluminescence of Charged CdSe/ZnS Quantum Dots in the Gas Phase: Effects of Charge and Heating on Absorption and Emission Probabilities

Collin R. Howder, Bryan A. Long, David M. Bell, Kevin H. Furakawa, Ryan C. Johnson, Zhiyuan Fang, and Scott L. Anderson*

Department of Chemistry, University of Utah, Salt Lake City, Utah 84112, United States

ABSTRACT Gas phase spectral measurements for CdSe/ZnS core/shell nanocrystal quantum dots (QDs) before and after heating with both infrared (CO_2) and visible lasers are reported. As-trapped QDs are spectrally similar to the same QDs in solution; however their photoluminescence (PL) intensities are very low, at least partly due to low absorption cross sections. After heating, the PL intensities brighten by factors ranging from ~4 to 1800 depending on the QD size and pump laser wavelength. The emission spectra no longer resemble solution spectra and are similar, regardless of the QD diameter. Emission extends from the pump laser wavelength into the near-IR, with strong emission features above the band gap energy, between 645 and 775 nm, and in the near-infrared. Emission spectra from brightened QD ensembles, single QD aggregates, and single QD monomers are similar, showing that even single QDs support PL from a wide variety of states. The heating and cooling processes for QDs in this environment are analyzed, providing limits on the magnitudes of the absorption cross sections before and after thermal brightening. A model, based on absorption bleaching by extra electrons in the conduction band, appears to account for the changes in absorption and emission behavior induced by charging and heating.

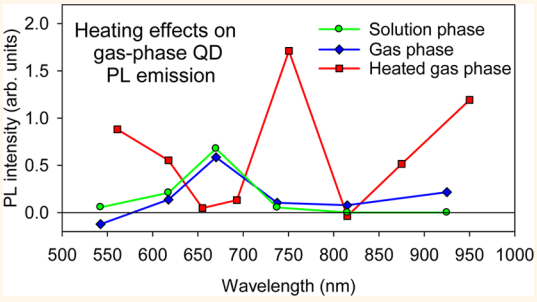

KEYWORDS: quantum dots · ion trap · single particle · mass spectrometry

Accurate, nondestructive mass determination for trapped nanoparticles (NPs) enables a number of interesting experiments, such as measuring kinetics for NP surface reactions by monitoring mass *vs* time as an NP is heated or exposed to reactants[1] or studying spectral properties of single NPs in the gas phase. Several groups have reported experiments wherein single NPs were trapped in a quadrupole (Paul) trap,[1−4] with continuous determination of the mass (*M*) and charge (*Q*) by monitoring the motional frequency of the trapped NP. For large NPs, motion is easily monitored by scattering of a low-power laser focused through the trap, and NPs that are too small for detection by light scattering (<~50 nm) can be monitored by photoluminescence (PL), provided they have significant PL quantum yields. Unfortunately, many interesting systems, such as small NPs of catalytically interesting metals, meet neither of these requirements. We are developing an approach to mass analysis of small "dark" NPs based on cotrapping with one or more small photoluminescent probe NPs, which must have reasonably strong, nonblinking PL that is stable under laser pumping for many hours, even when heated.

As shown recently,[5] CdSe/ZnS core−shell quantum dots (QDs) appear to meet all these requirements, but only after they have been "brightened" by laser heating. The observation that PL intensity increases by factors of up to 1000 after intense laser heating is counter to the usual experience for QDs in the condensed phase, and the motivation for this report is to examine the nature of the thermal brightening process. We report emission spectra and intensities for a variety of as-trapped and laser-heated QDs pumped at different wavelengths,

* Address correspondence to Anderson@chem.utah.edu.

Received for review September 22, 2014 and accepted November 26, 2014.

Published online November 26, 2014
10.1021/nn505374d

explore the effects of buffer gas pressure on the brightening process, discuss thermal balance in the laser-heated QDs, and derive estimates of gas phase QD absorption cross sections and emission quantum yields before and after heating. In addition to our own application, the laser-brightened QDs may prove useful in other applications where a robust luminescent probe is needed, capable of functioning over a wide temperature range.

QDs are widely used as fluorescence markers in the condensed phase, and their photophysics in the condensed phase have been studied in great detail.[6−8] In brief, QDs have a near continuum of electronic states in their valence and conduction bands, which are separated by a band gap. The band gap of QDs decreases with increasing diameter, such that large QDs absorb and emit lower energy photons than small QDs. Photons with energy exceeding the band gap energy are absorbed, pumping an electron into the conduction band and creating a hole in the valence band. The exciton relaxes and then recombines, resulting in emission of a photon with energy equal to the band gap energy. Current synthetic techniques yield QDs whose fluorescence quantum yield (QY) approaches unity.

Few observations of gas phase QD photophysics have been made, with the notable exception of Xiong *et al.*, who studied the photoelectron spectrum of a beam of QDs in the gas phase, directly probing the density of states.[9] Here we present a study of trapped gas phase QD photophysics before and after QDs are heated. Before heating, as-trapped QDs are only weakly emissive, but with spectra that are superimposable on the solution phase spectrum of the same QDs. Heating, either with a CO_2 or visible laser, increases the brightness of trapped QD emission by factors of up to 1800 and causes dramatic changes in the emission spectrum, which becomes independent of QD size and has peaks to the blue of the band gap emission, in the red, and in the near-IR. The emission of QDs in the condensed phase is also altered by heating; however, the effect is mainly a red shift in the emission and a decrease in emission quantum yield, until, at sufficiently high temperature (~520 K), PL is totally quenched.[10−12] The effect is believed to be due to creation of surface sites that act as electron traps.

In our experiment, either single NPs or small ensembles of NPs are confined in a radio frequency quadrupole ion trap, where they can be studied nondestructively for long time periods, allowing repeated measurements of the PL emission spectrum before and after laser heating and accurate determination of the mass of the NP and its charge. As described elsewhere[1,13] and summarized in the Experimental Methodology section, there is a well-defined frequency for motion of charged NPs in a quadrupole trap, which is a function of the NP's mass-to-charge ratio (*M*/*Q*).

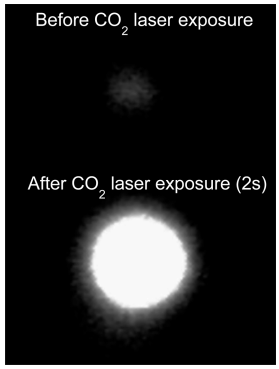

Figure 1. Images of a swarm of trapped QD NPs taken before (top) and after (bottom) heating by CO_2 laser irradiation.

M/*Q* can, therefore, be determined by measuring the motional frequency of the trapped NP, using PL to detect the motion. *Q* can be exactly determined by observing steps in *M*/*Q* induced by charge-changing collisions with ions or electrons in the buffer gas, and once *Q* is known, *M* is also determined. The PL emission spectra are measured by observing the emission through a series of long-pass filters.

To be trapped, the QDs in our experiments must be charged. We generate positively charged QDs with charges between $+5e$ and $+20e$ per QD using electrospray ionization (ESI). Charging[14−16] or doping[17−19] of QDs has been shown to have a significant impact on PL because the charge (either positive or negative) interacts with the exciton. In ESI the excess charge (excess Na^+ in this case) is confined to the surface of the NP. The effect of ESI charging of CdSe/ZnS QDs was investigated by Barnes *et al.*,[20] who electrosprayed QDs, then immediately collected and dried them on a surface and analyzed the PL. For negative charging, they observed an emission blue shift of 60 meV and a decrease in PL lifetime as a result of an average charge of $-5e$. For positively charged QDs they observed PL properties similar to the solution phase. In our case, the NPs are isolated in a low-pressure buffer gas, which allows their mass and charge to be precisely determined.

In the following experiments, both QD monomers and NPs consisting of small aggregates of QDs are trapped. For particles where the mass, hence the identity, was determined, we will refer to the particle as a "monomer", "dimer", *etc*. In experiments where the mass was not determined, we will use the term "NP", which includes both monomers and small aggregates.

RESULTS AND DISCUSSION

Emission Spectra and the Effects of Thermal Brightening. Images of an ensemble of trapped, gas phase CdSe/ZnS QD based NPs before and after brightening are shown in Figure 1. An ensemble of ~100 NPs was trapped and pumped at 532 nm with ~153 W/cm^2,

with 10 mTorr of Ar buffer gas to help cool the NPs. As trapped, the emission intensity is barely detectable by the CCD even with a 2 s frame rate. The NP ensemble was then heated by CO_2 laser irradiation (10.6 μm) for 2 s at an estimated intensity of ~1 kW/cm^2 and then reimaged with the CCD after the CO_2 laser was turned off. It can be seen that two seconds of heating led to a dramatic brightening of the QD NP emission intensity. This brightening is irreversible; that is, it does not decay if the NPs are trapped in the dark or continuously irradiated in the visible or if the argon pressure is varied.

The primary goal of this paper is to understand the processes leading to the initially weak PL efficiency and the thermal-induced PL brightening. Important insights can be obtained by examining the emission spectra of different core size QDs, before and after CO_2 laser-induced brightening. In the following, we will refer to the QDs by the color of their solution-phase band gap emission: green (λ_{max} = 540 nm, d = 2.5 nm), yellow (λ_{max} = 575 nm, d = 3.9 nm), orange (λ_{max} = 605 nm, d = 4.2 nm), and red (λ_{max} = 650 nm, d = 5.5 nm). The diameters given do not include the 1 nm thick ZnS shells. QDs were capped with mercaptoundecanoic acid. In an ideal experiment, we would trap and measure the mass, charge, and emission spectrum for single QD NPs, before and after CO_2 laser irradiation. Unfortunately, the emission from as-trapped, unbrightened NPs is far too weak to allow measurements on single NPs. Therefore, the as-trapped spectra are all for small ensembles of NPs. The mass and charge determination method does not work for ensembles; therefore we cannot directly determine what type of NPs are in the trap. After brightening, the intensities are sufficient to record PL spectra for both ensembles and single NPs, and for the latter, we can determine the mass and charge unambiguously.

532 nm Excitation. Figure 2 shows emission spectra for four different color QD NPs, all pumped at 532 nm. The six-point emission spectra presented here were measured using a series of long-pass color filters that can be inserted into our optical detection path (see Experimental Methodology). The vertical dashed lines are the cutoff wavelengths for each of the filters used, and the data points centered between the cutoffs represent the integrated emission intensities in each wavelength range, determined by subtracting intensities measured through the series of filters. In each frame, spectra are shown for the QD NPs in methanol solution, for small ensembles of as-trapped, unbrightened NPs, and for the same ensembles after CO_2 laser irradiation.

The spectra of as-trapped NPs were obtained using 532 nm pump laser intensities between 70 and 125 W/cm^2 and argon buffer pressures between 5 and 25 mTorr, with conditions optimized to minimize heating, avoiding unwanted brightening. (The visible

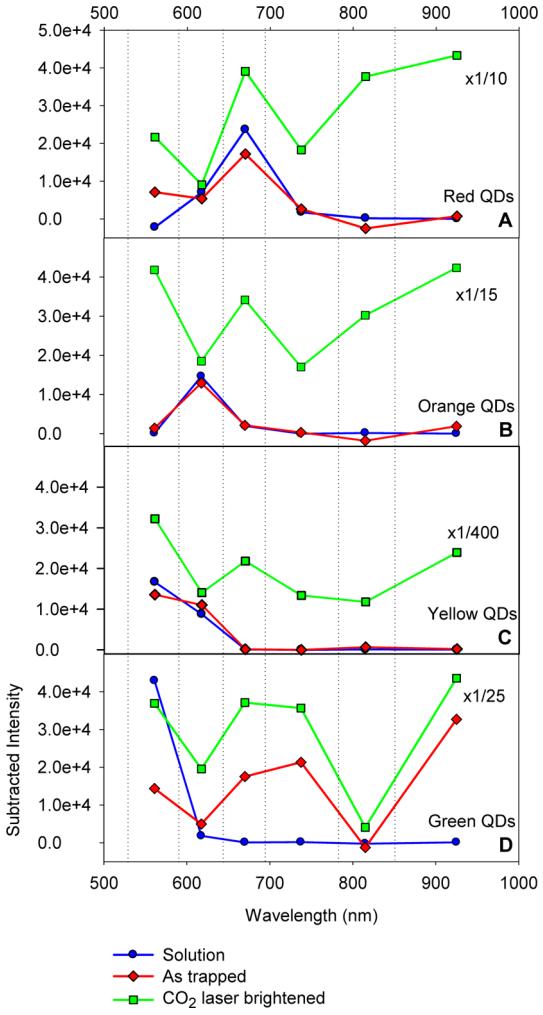

Figure 2. Emission spectra of swarms of red (solution λ_{max} = 650 nm), orange (solution λ_{max} = 605 nm), yellow (solution λ_{max} = 575 nm), and green (solution λ_{max} = 540 nm) trapped QD NPs pumped at 532 nm before (red) and after (green) heating by CO_2 laser irradiation. Dotted vertical lines are the cutoff wavelengths of the long-pass filters used, and the points represent the PL intensity in each wavelength range. Solution phase spectra (blue) measured with the same optical setup are included for comparison.

pump laser also heats the NPs, because only a fraction of the absorbed energy is re-emitted.) It is important to note that the experiments were done by injecting NPs into the trap while monitoring PL emission at low pump laser intensity, continuing injection until a signal level of at least 50 counts/s was observed, typically taking less than 5 s. As a result, the size of the ensembles examined should have been roughly inversely proportional to the PL efficiency for the particular combination of QD color and pump laser intensity. For combinations where the as-trapped PL is relatively efficient, fewer than 10 NPs provided sufficient intensity, but for combinations with very low PL efficiency, there may have been hundreds of NPs in the trap. Once an appropriate ensemble was trapped, the "as-trapped" emission spectrum was taken using the filter set, and then the ensemble was

exposed to the CO_2 laser at 1 kW/cm^2 for ~5 s, thereby increasing the fluorescence intensity by factors ranging from 55 to 1800. After turning off the CO_2 laser, the "CO_2 laser-heated" emission spectrum was taken, and then the NPs were ejected from the trap to allow measurement of a background spectrum for the empty trap. The background subtraction process is not perfect, resulting in occasional points with negative background-subtracted intensities. These are within the expected repeatability of the spectra (Figure S1, Supporting Information) and give an idea of the uncertainty inherent to the low signal levels for the as-trapped spectra.

To obtain the as-trapped spectrum for red QD NPs (QDs with 5.5 nm core diameter) shown in panel A, the NPs were injected into the trap with an argon buffer pressure of 15 mTorr with the 532 nm laser blocked. The pressure was then lowered to 10 mTorr, the NPs were exposed to the 532 nm laser at ~80 W/cm^2, and the emission spectrum was recorded. The total (unfiltered) photon count rate was ~300 counts/s. Note that the spectrum of as-trapped red QD NPs in the gas phase is quite similar to the spectrum recorded using the same method for the QD NPs in methanol solution, with a peak between 645 and 695 nm consistent with the manufacturer's reported emission spectrum (nominal λ_{max} = 650 nm). For the as-trapped spectrum, ~75% of the total emission is in the range expected for band gap emission, and most of the rest comes in a feature between 532 and 590 nm that is not present in the solution spectrum. This feature suggests there are emissive states in the as-trapped NPs with energies above the band gap. Although we made every effort to minimize the temperature of the as-trapped NPs, we cannot exclude the possibility that this above-band-gap emission was the result of heating by the PL laser. Note that the solution spectra in Figure 2 have been scaled so that their integrated intensities match those for the as-trapped ensembles, to allow the spectra to be compared directly. It is not possible to directly compare the absolute intensities, because even in the dilute methanol solution the number of NPs in the detection volume is ~10^5 to 10^6 times larger than in the trap, and the emission was so bright that the spectrum was collected without lenses used collect and focus emission from the trap. In principle, we could dilute the solution to obtain an NP density comparable to that in the trap; however, the dilution would be so large that issues such as NPs sticking to the cuvette walls would make the comparison useless.

After exposure to the CO_2 laser, the total emission intensity increased by a factor of 55, and the spectrum changed significantly. The emission in the band gap region between 645 and 695 nm increased by a factor of 20, as did the above-band-gap feature (532−590 nm), but the spectrum is dominated by emission in the near-IR, between 780 nm and the 1000 nm APD cutoff. (Note: The spectra are weighted by count rate, rather than emitted energy.) Even with our low spectral resolution, it is clear that there are *at least* three main emission features for the brightened ensemble, and the emission level is still well above background in the two spectral ranges between the three emission maxima. Clearly, IR heating of the NPs created a wide variety of emitting states. See below for higher resolution spectra of single red QD monomers.

The experiments for orange (panel B; 4.2 nm core dia.), yellow (panel C; 3.9 nm core dia.), and green QD NPs (panel D; 2.5 nm core dia.) were done similarly. For orange QD NPs a 532 nm laser intensity of 80 W/cm^2 was used with an argon pressure of 10 mTorr. The as-trapped and solution spectra are in near-perfect agreement, with a feature between 590 and 645 nm consistent with the expected band gap emission (nominal λ_{max} = 605, width 20 nm). IR heating increased the total photon count rate by a factor of ~160. After heating, the spectrum of the brightened orange QD NPs no longer had a maximum corresponding to band gap emission and instead had a structure quite similar to the spectrum of the CO_2 laser-heated red QD NPs, but with the intensity distribution weighted more strongly at shorter wavelengths, *i.e.*, higher intensity in the 532−590 nm range, with less in the near-IR. For yellow QD NPs (panel C), it was necessary to increase the 532 nm laser intensity to ~180 W/cm^2 to obtain sufficient emission signal (with 10 mTorr of argon buffer gas). Despite the higher pump laser intensity, the as-trapped spectrum is superimposable on the solution spectrum. In both cases, the emission peaks at the blue end of the spectrum, as might be expected given the fact that the solution emission maximum reported by the supplier (λ_{max} = 575 nm) is close to the 532 nm pump wavelength. After CO_2 laser heating, the total emission intensity increases by a factor of ~1800, and again, the brightened spectrum has features similar to those for the brightened orange and red QD NPs, but with the intensities weighted even more toward the blue.

The situation is somewhat different for the green QD NPs (Figure 2D). The manufacturer indicates that the solution phase emission spectrum for these runs between 520 and 550 nm and the first maximum in the absorption spectrum are shifted roughly 30 nm to shorter wavelength. Therefore, the 532 nm pump laser is able to excite only that fraction of the population with the reddest absorption spectra. As expected, the solution spectrum has significant emission only in the 532−590 nm range. It proved impossible to obtain an unbrightened spectrum for these QD NPs with the 532 nm pump laser, and the dependence of emission intensity on pump laser intensity provides additional insight. As the intensity was gradually increased, the emission was undetectable (<20 counts/s) until the intensity reached ~100 W/cm^2, at which point the

emission suddenly jumped to ~900 counts/s. We then took the "as-trapped" emission spectrum shown in Figure 2D, which looks nothing like the solution spectrum. Upon CO_2 laser heating, a further increase in intensity by a factor of ~50 occurred, with essentially no change in the emission spectrum, suggesting that the "as-trapped" spectrum was actually for NPs that had been heated and brightened by interaction with the 532 nm laser. On the basis of experiments and simulations discussed below, thermal brightening of QD emission appears to be an all-or-nothing effect; that is, individual NPs cannot be partially brightened. Therefore, the factor of 50 increase in emission from CO_2 laser heating suggests that ~2% of the as-trapped ensemble were brightened by the 532 nm laser (presumably those with the reddest absorption spectra), and the rest were brightened upon CO_2 laser heating.

445 nm Excitation. On the basis of the behavior of the green QD NPs with 532 nm excitation, we would expect to be able to obtain an as-trapped, unbrightened spectrum for the green QD NPs using a bluer pump laser. As shown in panel B of Figure 3, this is correct. An ensemble of green QD NPs was trapped in 15 mTorr of Ar with the laser blocked. The pressure was then raised to 20 mTorr and V_0 was lowered from 500 to 450 V before exposing them to the 445 nm pump laser at ~125 W/cm^2 intensity. Because the photon energy and the emission Stokes shift are higher when pumping at 445 nm, the heat load on the NPs is higher. The higher argon pressure helps collisionally cool the NPs, and the lower V_0 also helps by allowing the ensemble volume to expand, such that each NP spends a smaller fraction of the time in the laser focus. The as-trapped spectrum is in excellent agreement with the solution spectrum, with a single emission feature in the 495−590 nm range (limited by the 495 nm long-pass filter used to block scattered laser light), consistent with the nominal band gap emission (λ_{max} = 540 nm). The effect of CO_2 laser heating on the NPs was qualitatively similar to that seen with the 532 nm pump laser: a new feature grew in in the 645−695 nm range, but the brightened spectrum was dominated by near-IR emission. The total intensity increase in this case was only a factor of ~6.

Panel A of Figure 3 shows 445 nm laser pumping of the red QD NPs. The as-trapped and solution phase spectra are essentially identical, and then after CO_2 heating, significant new intensity grew in both to the blue of the original peak and in the near-IR. The brightened spectrum is quite similar to that seen for the red QD NPs with 532 nm pumping; however, the intensity increase from CO_2 laser heating was only a factor of 4, compared to a factor of 55 for 532 nm pumping.

The similarity of all the brightened spectra suggests that heating, by either the CO_2 or 532 nm lasers, creates

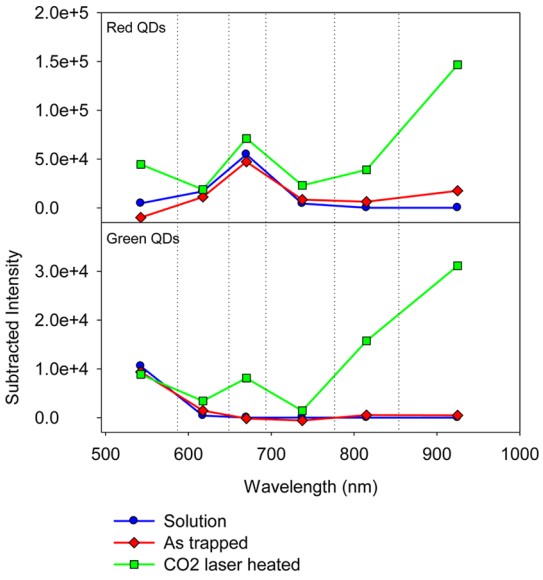

Figure 3. Emission spectra of swarms of red (solution λ_{max} = 650 nm) and green (solution λ_{max} = 540 nm) trapped QD NPs pumped at 532 nm before (red) and after (green) heating by CO_2 laser irradiation. Solution phase spectra (blue) measured with the same optical setup are included for comparison.

new states in the NPs, and the fact that the spectra are similar, independent of QD diameter/band gap energy, indicates that the emission is no longer primarily from exciton recombination in the QD cores.

Single QD NP Emission Spectra. The emission spectra in Figures 2 and 3 show that small ensembles of CO_2 laser-heated QD NPs emit over a wide wavelength range, extending from the pump wavelength to at least the near-IR. There are clear maxima in the spectra, independent of the QD size, suggesting that there are at least three main emission features. One obvious question is whether the complex emission spectra simply result from heterogeneity in the ensemble of CO_2 laser-heated NPs or if each QD supports emission from many states.

Figure 4 shows one approach to answering this problem. After completing the CO_2 laser brightening experiment on the small ensemble of red QD NPs (Figure 3A), the emission of the ensemble was studied with 445 nm excitation as NPs were selectively ejected from the ensemble. In the following the axial component of the secular frequency is denoted f_z. Figure 4A shows the f_z spectrum of the ensemble, obtained by monitoring PL while applying a 250 mV sinusoidal drive potential to one of the trap end-cap electrodes, sweeping the frequency from 20 kHz to 1 kHz. Dips in the PL signal are expected when f_{drive} is resonant with f_z for one or more of the NPs. In this case, the dips at 7.5, 9.5, 11, and 12 kHz indicate there were NPs with M/Q around ~180, ~140, ~120, and ~110 kDa/e. The breath of some of the resonances suggests that more than one NP contributes to some of these features, and based on the signal changes during the ejection

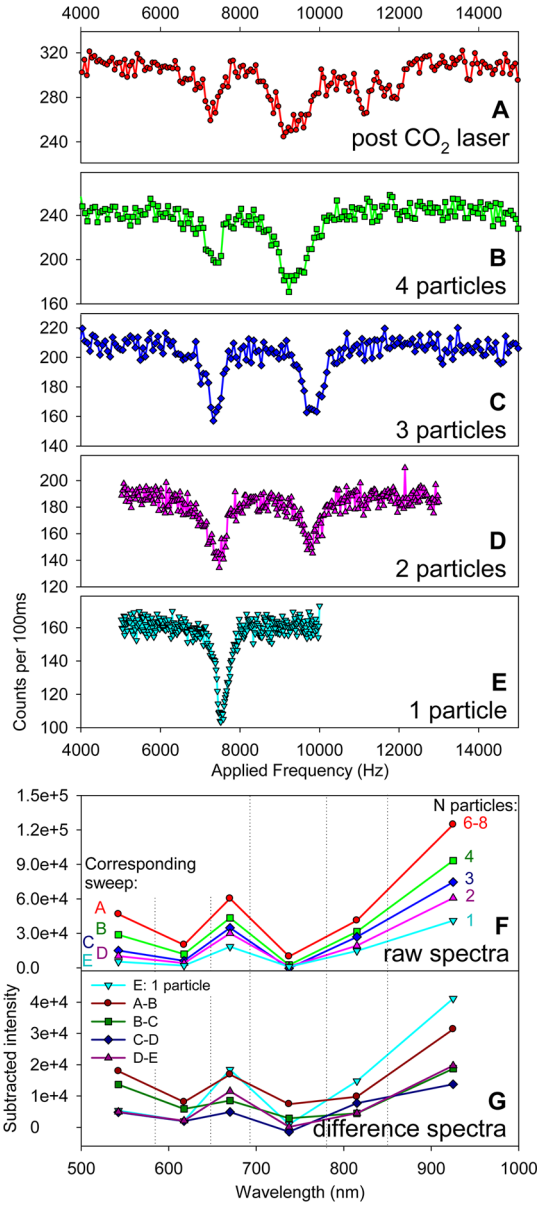

Figure 4. Frequency spectra for a swarm of trapped red (solution λ_{max} = 650 nm) QD NPs as NPs were selectively ejected. (A) Immediately after thermal brightening with an estimated 6−8 NPs in the trap, (B) 4 NPs, (C) 3 NPs, (D) 2 NPs, (E) 1 NP. (F) Emission spectra corresponding with the sweeps. (G) Subtracted emission spectra, which approximate single NP spectra.

experiment, we estimate that the initial ensemble contained 6−8 NPs. The corresponding emission spectrum, identical to that in Figure 3A, is shown in Figure 4F ("A").

Frames B−E of the figure show the f_z spectra as NPs were selectively ejected from the trap, working from the high-f_z (low M/Q) end of the spectrum. Frame B shows the f_z spectrum obtained after high drive potential was applied at 12 kHz, ejecting the NPs giving rise to both the 11 and 12 kHz f_z resonances. The associated emission spectrum is shown in panel F of the figure, labeled "B". At this point, only two features remained in the f_z spectrum; however, from the breath of the feature at ∼9 kHz, we suspected that more than one NP was contributing. Frame C and the spectrum labeled "C" in frame F show the result of applying a 9.5 kHz drive signal for 3 s, starting with 1 V amplitude and then increasing the amplitude in 500 mV steps until an irreversible decrease in emission intensity signaled that one or more NPs had been ejected. This process was then repeated to obtain the f_z spectrum in frame D and emission spectrum labeled "D" and then again to obtain the f_z spectrum in frame E and emission spectrum labeled "E". Note that as NPs were selectively ejected, the relative intensity of the 9 kHz feature progressively decreased and its width narrowed. It can be seen that the final single NP emission spectrum is, apart from intensity, almost identical to the emission spectrum of the initial ensemble, demonstrating that a single NP can support emission from many different states.

The approximate numbers of NPs remaining in the trap at each stage of the ejection process were estimated from the PL intensity changes; however, the fact that only a single NP remained at the end is unambiguous. The f_z spectrum (analogous to frame E) was recorded repeatedly as the NP was excited by the PL pump laser for ∼16 h. Figure S2 in the Supporting Information shows how f_z for this NP changed with time, as the NP underwent a series of charge-changing collisions with Ar^+, Ar* metastables, or electrons. The trapping conditions were changed somewhat from those used for Figure 4, resulting in a higher f_z and a narrower f_z resonance. If the trap had contained more than one NP, which by coincidence happened to have nearly identical f_z at the start of the experiment, this would have resulted in development of multiple resonances as the NPs changed charge. From the step sizes the absolute charge, Q, can be determined (integers indicated on the figure), and then the absolute mass (3.26 MDa) is easily obtained using eq 1. The ∼10% change in apparent mass over the 16 h is attributed mostly to slow mass loss due to heating by the PL laser, although we cannot rule out a contribution from drift in the trapping conditions, because the rf generator used in these experiments was not stabilized. Nonetheless, 10% mass accuracy is still far better than the factor of ∼2 mass spread of the stock QDs, which only allows us to say that the NP was an aggregate containing 4 to 7 QDs, with a charge between +3e and +6e per QD at the beginning of the observation time.

The fact that this final NP was an aggregate is not surprising, because the ejection process selectively retained the NP with the highest M/Q (180 kDa/e). This, however, obviously raises the question of whether the ability of this single NP to support emission from many different states is simply a function of it being an aggregate. The answer is "no", as shown by several experiments. First, by examining the differences

between the spectra taken at different steps in the ejection process, it is possible to see what the spectra look like for each of the ejected NPs, as shown in panel G of Figure 4, which compares the emission spectrum of the final aggregate NP (E: 1 NP) with the difference spectra, *i.e.*, the spectra of the ejected NPs. It is clear that the emission spectra have hardly any dependence on M/Q. For example, the A−B difference spectrum, for two NPs with $M/Q = 110$ and 120 kDa/e, is quite similar to the spectrum for the final $M/Q = 180$ kDa/e aggregate. While there are small variations in the relative intensities emitted in the different wavelength ranges, all the difference spectra are qualitatively similar.

A more definitive answer is provided in Figure 5, which shows the emission spectra for what are clearly monomeric QDs. This experiment was done using a different approach, where short pulses of red QD NPs were injected into the trap with both the CO_2 laser and 532 nm PL laser on, so that brightening would occur immediately. As soon as an emission signal was observed, the CO_2 laser was turned off, and the secular frequency spectrum was measured to verify that only a single NP was trapped. The emission spectrum was measured, and then charge stepping was monitored in order to determine the mass and charge. In addition, for these experiments, several additional filters were used to improve the spectral resolution.

Emission spectra are shown for two monomers, the first with a mass of 595 kDa with $+18e$ charge and the second with a 740 kDa mass with $+14e$ charge. From the reported ~±10% diameter distribution of the stock red QDs used in this experiment, we can estimate that the mass range for QD monomers should be ~460 to ~860 kDa. The 595 kDa particle is, therefore, clearly a monomer. The 740 kDa particle could conceivably be a dimer of two monomers that both happened to be at the extreme small end of the stock size distribution; however, it is much more likely that this, too, is a monomer. In both cases, the spectra show three clear emission features, with near-zero intensity in between. One feature is to the blue of the excitonic emission (650 nm for these QDs; Figure 2A), one peaks between 720 and 775 nm, and the final feature is in the near-IR, probably peaking beyond the sensitivity range of our avalanche photodiode detector (APD).

For reference, the bulk band gap of CdSe at 300 K is 1.74 eV,[21] corresponding to emission at 713 nm. The two spectra are quite similar and are also similar to the ensemble spectrum (Figure 2A) for NPs prepared from this size QD.

We cannot rule out the possibility that NPs that are aggregates of QDs might become hot enough under laser heating to partially or completely fuse, forming a particle with larger effective diameter. Note, however, that the emission spectra after heating/brightening do not appear to depend on QD diameter (Figures 2 and 3), are similar for aggregate NPs (Figure 4) and QD

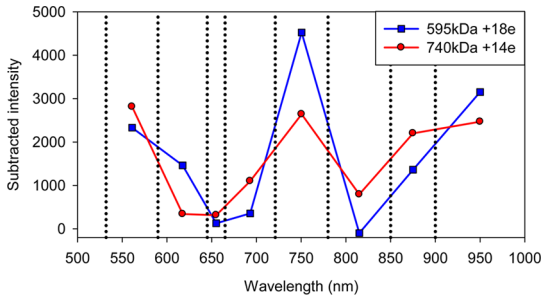

Figure 5. Single trapped red QD monomer emission spectra (solution λ_{max} = 650 nm). No emission is observed at 650 nm, indicating excitonic emission is totally bleached.

monomers (Figure 5), and all have features well to the red of even bulk CdSe band gap emission. Therefore, we conclude that fusion to form larger particles is not responsible for the emission red shift, and conversely, the emission spectra would probably not be sensitive to fusion.

Another obvious question is whether the near-IR emission observed for all the QD NPs at both pump wavelengths is really PL or if it could be partially or entirely thermal emission due to heating of the NPs by the PL pump laser. To investigate this issue, a single NP formed by ESI of red QDs was trapped and monitored with 532 nm excitation, and the charge-stepping procedure was used to determine that its mass was 1.76 MDa and that it had charge $Q = +23e$ at the beginning of the series of charge steps. From the mass, this NP is an aggregate, probably a trimer. The emission spectrum was then measured repeatedly, varying both the 532 nm laser intensity and the argon pressure, looking for any increase in near-IR emission under conditions where the QD aggregate would tend to be hotter (high laser power, low buffer gas intensity). As might be expected, no change was seen. The fact that the QD aggregate was stable over the course of the hour needed to measure six emission spectra implies that the particle temperature must have remained well below the sublimation temperature. The bulk sublimation temperature for ZnS is 1450 K,[22] and CdSe melts and decomposes at ~1540 K;[23] however, the vaporization temperature should be significantly lower for small particles in a vacuum. For example, electron microscopy experiments[24] showed sublimation of CdSe/CdS nanostructures on the hour time scale, at temperatures of only ~873 K. In this temperature range, less than 10^{-4} of the radiated power is at wavelengths below 1000 nm, and a single NP would emit only ~500 photons/s in the <1000 nm range, assuming an emissivity of 1.0. In reality, subwavelength diameter particles have emissivities well below unity,[25−29] and the thermal emission rate for $\lambda < 1000$ nm would be too small to detect, given the ~1% efficiency of our photon detection system. The NP temperature is discussed further below.

Photoluminescence before and after Heating: Why Emission for As-Trapped QD NPs Is Weak. The results of these

experiments show that ensembles of unheated, charged NPs in the gas phase show excitonic emission spectra, similar to those for the same NPs in methanol solution, but with much lower intensity. Upon heating, the emission brightens substantially, but the spectra no longer look excitonic. One question is whether the low emission signal for as-trapped NPs results from low PL quantum yields, from small absorption cross sections, or from some combination of both factors. It is useful to consider two limiting cases.

First, consider the case where the absorption cross section (σ_{abs}) is assumed to be similar to that for the same QDs in solution. Solution phase σ_{abs} values have been reported in the literature for a variety of QDs excited over a wide range of wavelengths.[30−33] For the QDs and pump wavelengths used here, the solution phase absorption cross sections would be in the range between $\sim 2 \times 10^{-15}$ cm^2 (green QDs pumped at 532 nm) and $\sim 1 \times 10^{-14}$ cm^2 (red QDs pumped at 445 nm).

Consider the ensemble spectrum of red QD NPs pumped at 445 nm (Figure 3A). The selective ejection experiments outlined in Figure 4 allow us to estimate that there were ~6 to 8 NPs in the trap. From the emission measured before CO_2 laser exposure, we can estimate, taking the light detection efficiency into account, that the average emission/NP in the unheated NP ensemble was ~8700 photons/s at 125 W/cm^2 of 445 nm pump intensity. At least some of the NPs in this ensemble were aggregates, and for the purpose of estimating σ_{abs}, we will assume that the average aggregate size was 3 QDs. For the unheated NPs, we might expect that σ_{abs} for such a particle might lie between 1 and 3 times the cross section for a red QD monomer at 445 nm (*i.e.*, $\sim 10^{-14}$ cm^2). Such NPs would absorb $\sim 3 \times 10^6$ photons/s/NP; thus the ~8700 photon/s/NP emission level would imply a PL QY of only 0.3%. If, instead, we assume that QY = 1, then σ_{abs} would need to be ~0.3% of the solution phase value, or $\sim 3 \times 10^{-17}$ cm^2.

Thermal Balance in Gas Phase QD NPs under Visible Laser Excitation. Thermal considerations allow us to set a maximum on the magnitude of σ_{abs} for the as-trapped NPs. Consider the limit where the as-trapped QD NPs have σ_{abs} equivalent to those measured in solution, with small QY. The highest absorption cross section would be for red QD NPs pumped at 445 nm (solution $\sigma_{abs} \approx 1 \times 10^{-14}$ cm^2),[33] and for 125 W/cm^2 laser intensity (conditions of Figure 3A), the absorption rate would be $\sim 2.8 \times 10^6$ photons/s, giving rise to a heating rate of $\sim 8 \times 10^6$ eV/s = $\sim 1.2 \times 10^{-12}$ W. At the other extreme, yellow QD NPs under the conditions of Figure 2C, *i.e.*, pumped by 180 W/cm^2 of 532 nm (solution σ_{abs} $\sim 2 \times 10^{-15}$ cm^2), would absorb $\sim 1 \times 10^6$ photons/s, corresponding to a heating rate of 2.2×10^6 eV/s, or 3.6×10^{-13} W.

The NP temperature is determined by the balance between the heating rate and the sum of all cooling processes, including photoluminescence, thermionic emission of electrons, evaporation, thermal emission of photons, and buffer gas collisions. Because the emission QY is assumed to be low in this scenario, the photoluminescence cooling is negligible, and the fact that the charge/NP does not increase rapidly during the experiments shows that thermionic emission of electrons is also negligible from a cooling perspective. For any reasonable estimate of the enthalpy of sublimation (*e.g.*, ΔH_{subl} = 321.7 kJ/mol for bulk CdSe = ~3.3 eV/atom)[34] many thousands of atoms would have to sublime *per* second to contribute significantly to cooling, but the actual sublimation rates under conditions used here are less than 1% of the NP mass per hour (*e.g.*, Figure S2), corresponding to ≤0.1 atom/s. The only significant cooling mechanisms are buffer gas collisions and thermal photon emission.

The flux-weighted energy transfer per buffer gas collision is $2k(T_{surface} - T_{gas})c_A$, where $T_{surface}$ is the NP surface temperature, T_{gas} is 300 K, and c_A is the energy accommodation coefficient (a measure of inelasticity). Energy accommodation in collisions of argon with surfaces is expected to be reasonably efficient. For example, the accommodation coefficient for Ar colliding with a heated tungsten surface is ~0.25,[35] and it should be larger for collisions with ZnS because the surface atom masses are lower.[36] From the perspective of the as-trapped NPs, collisions would be with the ligand layer, and based on scattering measurements for Ar from organic surfaces,[37,38] c_A for 300 K Ar should be close to unity. Accommodation for helium is expected to be lower; however, the collision rates for a given pressure are also higher. The total collision rate, and therefore the cooling power, is linear with buffer gas pressure. Figure 6A shows the collisional cooling power (W/NP) as a function of $T_{surface}$, calculated for a 7.5 nm diameter spherical NP in 6, 10, and 60 mTorr of Ar and He, assuming c_A = 1 and 0.2, respectively.

The cooling rate from thermal emission of photons can be estimated from the Stefan−Boltzmann law: $P(W/m^2) = \sigma\epsilon(T_{surface}^4 - T_{gas}^4)$, where σ is the Stefan−Boltzmann constant and ϵ is the emissivity. Subwavelength-diameter particles have emissivities well below unity.[25−29] Figure 6B plots the cooling power as a function of $T_{surface}$ for ϵ = 0.01, 0.05, and 0.1, covering the range expected for 5−10 nm NPs. It can be seen that for low temperatures collisional cooling dominates, but for high temperatures, radiative cooling becomes increasingly important. Figure 6C gives the sum of the collisional and thermal photon cooling rates for Ar at 6 and 60 mTorr pressure, assuming ϵ = 0.01 and 0.1, *i.e.*, covering the ranges relevant to our experiments.

Thermal Constraints on σ_{abs} for QD NPs before and after Heating. With this understanding of the thermal balance in QD NPs under laser irradiation, it is possible to put some limits on the magnitude of σ_{abs}. If we assume

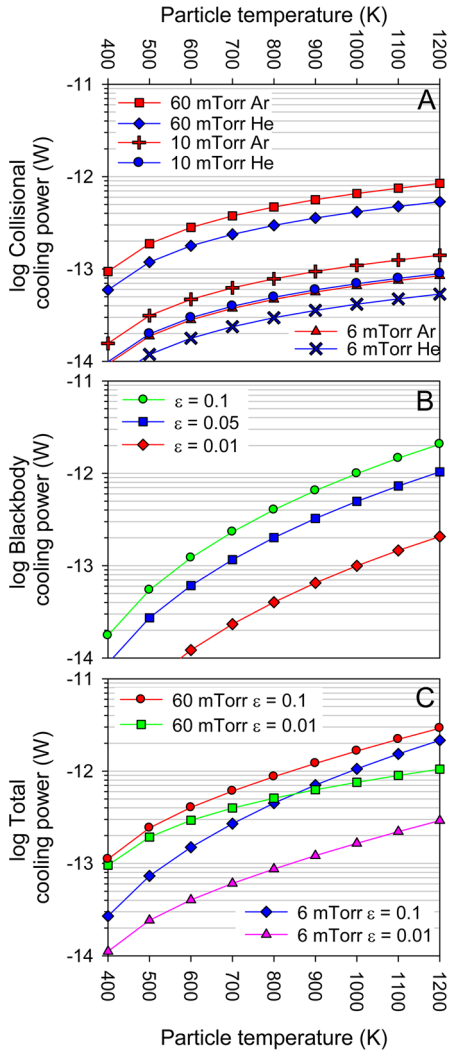

Figure 6. Simulated cooling powers for a trapped 7.5 nm particle under the range of conditions relevant to our experiments: (A) Gas collisional cooling power, (B) blackbody cooling power, and (C) the total cooling power.

solution-like σ_{abs} for the as-trapped NPs, the heating rate for red QD NPs pumped by 125 W/cm^2 of 445 nm radiation in 20 mTorr of Ar (the conditions of Figure 3A) is 1.2 $\times$ 10^{-12} W. The total cooling rate matches the heating rate only at temperatures between ~1030 K (assuming ϵ = 0.1) and ~1800 K (ϵ = 0.01). For yellow QD NPs pumped with 180 W of 532 nm in 10 mTorr Ar pressure (conditions of Figure 2C, 3.6 $\times$ 10^{-13} W), the steady state temperature would be between 720 and 1170 K, depending on the value assumed for ϵ. As already noted, CdSe nanostructures were observed by TEM to sublime on a much faster time scale than ours, at temperatures as low as 773 K. Furthermore, the mercaptoundecenoic acid surface layer would desorb or pyrolyze at even lower temperatures (see below). Therefore, the observation that as-trapped NPs have solution-like emission spectra that are stable for at least 20 min of continuous excitation, and that the sublimation rates are less than 0.1 atom/s, indicates that the NPs are not reaching even the lower range of the predicted temperatures.

Therefore, we conclude that σ_{abs} for the as-trapped QD NPs must be significantly smaller than typical solution phase cross sections. Presumably this factor also at least partially accounts for the weak emission observed. The actual σ_{abs} value must be small enough that the NPs do not reach temperatures that result in creation of surface (or core) defects that would significantly change the absorption/emission properties. It is not clear what temperature might be required to damage a thiol ligand layer on ZnS, but there is considerable information on the analogous gold thiol systems, and there is a theoretical prediction[39] that the $S_{thiolate}$—Au and $S_{thiolate}$—ZnS bonds should have similar energies. Lavrich *et al.*[40] used thermal desorption in a vacuum to study a variety of alkanethiols on Au(111) and found that chemisorbed molecules began to desorb around 450 K, with desorption peaking near 480 K, with corresponding desorption energies around 1.3 eV, independent of chain length. A similar study using mass spectrometric detection for cyclopentanethiol on Au(111) observed decomposition products starting at ~400 K, peaking near 440 K,[41] with masses suggesting that the C—$S_{thiolate}$ bond had broken. These experiments used heating rates of 2 and 1 K/s, and therefore we observed changes only when the desorption/decomposition time scale was shorter than ~20 s. Our experiment requires that the NPs be stable on a ~1000 s time scale. Zhao *et al.*[11] reported a study of thermal effects on the PL of CdSe/CdS/ZnS core/shell/shell QDs in solution and polymer matrices and found that PL intensity was irreversibly lost by ~423 K in solution, but that the polymer matrix reduced the temperature effects by preventing ligand loss. On the basis of these considerations, 450 K appears to be a safe estimate for the maximum temperature at which the as-trapped NPs might survive for 1000 s without desorption or damage to the ligand layer.

In order to keep red QD NPs below 450 K under the conditions of Figure 3A, σ_{abs} would have to be less than ~1.5% to 4% of the solution cross section for ϵ assumed to be in the 0.01 to 0.1 range. Similarly, for yellow QD NPs under the conditions for Figure 2C, σ_{abs} would have to be less than 16% to 35% of the solution σ_{abs}, depending on the value assumed for ϵ. In fact, we will argue below that σ_{abs} for the as-trapped QD NPs must be even smaller than these upper limits.

Comparison of σ_{abs} before and after Brightening. Further insight regarding the magnitudes of σ_{abs} before and after brightening can be obtained from the experiment shown in Figure 7. A small ensemble of red QD NPs was trapped in the dark at 7 mTorr pressure of Ar. The pressure was then raised to 60 mTorr, and the ensemble was exposed to 165 W/cm^2 of 532 nm laser, resulting in a stable, but very low level of emission. The pressure was then decreased slowly, until at ~6 mTorr, an abrupt

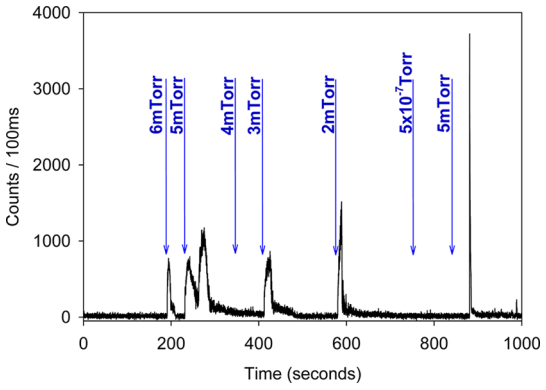

Figure 7. Thermal activation and rapid bleaching at high 532 nm laser intensity (165 W/cm^2) observed as a function of decreasing pressure. Visible irradiation brightened QD NPs in a narrow pressure range (6−2 mTorr). A certain set of NPs could not be brightened at pressures as low as 5×10^{-7} Torr, but were rapidly brightened as a result of CO_2 laser exposure at 5 mTorr.

onset of emission was observed. With the pressure held constant at 6 mTorr, the emission was observed to decay to baseline in ∼10 s. At that point, the pressure was again decreased until at 5 mTorr a second emission burst occurred, and before that had completely decayed, a third was observed while the pressure was still ∼5 mTorr. Further decreases in the pressure led to additional emission bursts at ∼3 and ∼2 mTorr, but then no further emission was observed as the pressure dropped to 5×10^{-7} Torr. At that point, the pressure was increased to 5 mTorr, and the CO_2 laser was focused through the trap at ∼1 kW/cm^2, leading to a final, short-lived burst of emission.

Our interpretation of this experiment is as follows. As discussed in conjunction with Figure 2C, emission from gas-phase QD NPs can be brightened by heating using either visible or CO_2 laser irradiation. As discussed above, however, as-trapped QD NPs have small σ_{abs}, such that at the high initial pressure collisional cooling was sufficient to keep the NPs below the temperature required to drive the brightening process ($T_{brighten}$). As the pressure was decreased, the temperature of the NPs increased, but because the ensemble included QDs with a distribution of sizes and spectral properties, the temperature rise would have been different for each NP. At pressures down to 6 mTorr, collisional cooling was sufficient to prevent any of the NPs from reaching $T_{brighten}$. As discussed above, if we assume this temperature to be 450 K, then we can put an upper limit on σ_{abs} (for the NP that absorbed most strongly), of between 1 and 3×10^{-16} cm^2 (for $\epsilon = 0.01$ and 0.1). That is less than a tenth of the estimated solution σ_{abs} for red QD NPs pumped at 532 nm (∼4×10^{-15} cm^2).[33]

At this point one of the NPs reached $T_{brighten}$, leading to a sudden jump in emission, which then bleached within ∼10 s. The process was repeated for additional NPs as the pressure continued to drop, as each NP's temperature reached $T_{brighten}$. The fact that there was an additional brightening event upon CO_2 laser irradiation indicates that a few NPs remained in the trap that had not brightened under the influence of the 532 nm laser. These presumably were QD NPs with absorption spectra shifted too far to the blue to significantly absorb at 532 nm, *i.e.*, QDs at the small end of the size distribution. The CO_2 laser is evidently able to heat such NPs, leading to brightening and then very rapid bleaching.

The bleaching process for gas phase QDs pumped at 532 nm has been studied previously.[5] In those experiments, a single green CdSe/ZnS QD NP was trapped, and its mass and emission intensity were monitored continuously as the particle was laser heated (at 532 nm) to drive slow sublimation over the course of several days. Periodically, the 532 nm power was lowered to allow measurement of emission intensity and spectra at a laser intensity where the particle mass was stable. It was found that the emission spectrum was quite stable even as the particle lost up to 85% of its initial mass and that emission intensity varied roughly as $M^{2/3}$, *i.e.*, as the surface area. The conclusion was that visible laser bleaching is simply due to sublimation, and if QDs are kept below the sublimation point, they exhibit emission that is stable indefinitely. In Figure 7, the combination of low buffer pressure and high 532 nm intensity resulted in rapid sublimation.

Knowing this, we can interpret the abrupt increase in emission and rapid bleaching to learn about changes that must be occurring in the σ_{abs}. As already noted, the fact that modest buffer gas pressures are sufficient to keep the NP temperature below $T_{brighten}$ implies that σ_{abs} for the as-trapped NPs must be small, between 1 and 3×10^{-16} cm^2. The abrupt brightening of emission when the temperature reached $T_{brighten}$ could be due to an increase in σ_{abs}, an increase in the emission QY, or some combination of the two. If only the QY increased, that would cool the NPs by radiating away a larger fraction of the absorbed photon energy, and in that case the NPs would be stable. Instead, the brightened QD NPs rapidly sublime, indicating that the temperature must increase substantially when the NPs brighten, implying that σ_{abs} must increase substantially. We can roughly estimate how hot the NPs must get to sublime within 10 s, based on the observation[24] that 40 nm CdSe/CdS octapods (with surface area/volume ratios similar to our QD NPs) sublime in ∼500 s at 873 K. If we assume that the sublimation rate is exponential in temperature, then the temperature required to drive sublimation 50 times faster is

$$T = (873^{-1} - k/E_{subl} \ln(50))^{-1}$$

where k is the Boltzmann constant and E_{subl} is the sublimation energy per atom. If we assume the bulk heat of sublimation of CdSe (3.3 eV),[34] T would need to be ∼950 K, and if a lower heat of sublimation is

assumed for NPs, then the temperature would need to be higher (*e.g.*, E_{subl} = 2.5 eV gives T = 990 K). The value of σ_{abs} required to reach 950 K under these conditions (6 mTorr, 165 W, 532 nm) would be between ~0.85 and 5 × 10^{-15} cm^2 for ϵ between 0.01 and 0.1. T = 990 K would require a cross section between ~1 and 7 × 10^{-15} cm^2, compared to the *upper limit* on σ_{abs} before brightening of 1 to 3 × 10^{-16} cm^2. The increase is at least an order of magnitude.

This increase in σ_{abs} also explains why brightening is so abrupt. As the NP begins to brighten, σ_{abs} increases, which leads to further increase in temperature, which further increases σ_{abs}, *etc.*, until a new steady state is established with high σ_{abs}, brighter PL, and NP temperature high enough to drive rapid sublimation. As shown in Figure 2A, the total PL intensity in the wavelength range below 1000 nm increased by a factor of ~55 for red QD NPs at 532 nm; thus it is possible that the brightening can be entirely attributed to an increase in σ_{abs}, although it seems more likely that both absorption and emission would be affected by changes to the QD NPs.

Why σ_{abs} Is Small in the As-Trapped State. Thermal considerations indicate that σ_{abs} for as-trapped QD NPs is considerably smaller than for the same QDs in solution, and the question is why. Important evidence is provided by the dependence on QD size and pump laser wavelength of the brightening factor, *i.e.*, the factor by which the emission brightens when the NPs are heated. The inset to Figure 8 shows the absorption spectra measured for green and red QD NPs diluted 1:100 in methanol (*i.e.*, our ESI solutions). The main figure shows the brightening factors, plotted as a function of the energy difference between the laser and absorption onset wavelengths, $\Delta E_{p\text{-}o}$. Brightening factors are shown for all QD/laser combinations in Figures 2 and 3, with the exception of green QD NPs pumped at 532 nm, where the unbrightened PL intensity was zero, corresponding to an infinite brightening factor.

The near-exponential dependence of the brightening factor on $\Delta E_{p\text{-}o}$, as well as the smallness of σ_{abs} for unbrightened QD NPs, suggests that the low-energy portion of the absorption spectra for the as-trapped NPs is bleached, such that the absorption onset energy is blue-shifted by ~0.2 to 0.3 eV compared to the solution phase onset. The onset wavelength for as-trapped green QD NPs would be shifted to ~520 nm (~580 nm in solution), explaining why the 532 nm laser could not excite PL (brightening factor = ∞). With increasing QD size, the absorption spectra shift to the red. For the yellow QDs, the solution phase absorption onset is at ~600 nm, but the proposed bleaching would shift this to 535 nm, such that the 532 nm laser would excite as-trapped yellow QD NPs, but very weakly (brightening factor =1800). The orange QDs have an onset at ~630 nm in solution, shifting to

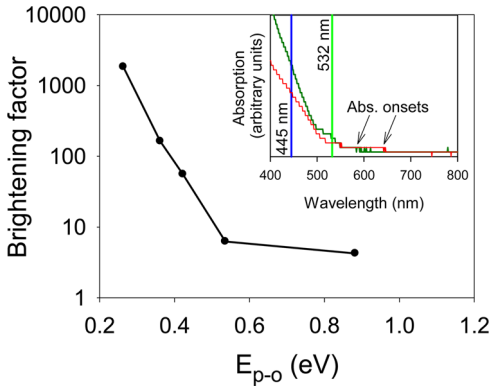

Figure 8. Brightening factor, the amount PL intensity increases as a result of thermal brightening, decreases as the difference between the pump energy and the absorption energy ($E_{p\text{-}o}$) increases. Sample absorption spectra are included as an inset.

~560 in the gas phase, resulting in somewhat stronger excitation of the as-trapped QD NPs, and a brightening factor of 160. The red QDs would have an as-trapped absorption onset at ~590 nm (650 nm in solution), and the expected stronger absorption at 532 nm explains why the brightening factor was only 55. The 445 nm pump laser would be well above the bleached spectral region for all the QDs, explaining why the brightening factors were only 6 (green QD NPs) and 4 (red QD NPs).

The QDs examined in this study are capped with mercaptoundecenoic acid, in a Na^+-containing buffer solution with a pH of ~8; that is, the acid groups should be mostly ionized, with the carboxylate negative charge balanced by Na^+. From typical ligand packing densities[42] we would expect ~50 ligands/QD. This solution was diluted in methanol and electrosprayed, producing QD NPs in the gas phase with a positive charge of 5*e* to 15*e* per NP. Under these conditions, the positive charge should almost entirely be due to excess Na^+, which we might expect to be mostly on the exterior of the ligand layer, complexed to carboxylate groups. Na^+ cations (recombination energy 5.1 eV[43]) located on the exterior of the ligand layer, at some distance from the surface of ZnS (work function ≈ 7.0 eV[44]), are unlikely to extract electrons from the semiconductor NP. In essence, however, the shell of excess cations establishes a positive potential on the semiconductor NP, which may result in attraction of electrons during the ESI process (counterbalanced by more Na^+). Excess electrons on the semiconductor NP would be most stable in the CdSe core, and thus would tend to populate states at the bottom of the conduction band. These excess electrons would block photoexcitation to the bottom of the conduction band,[14,16,17,45] bleaching the low-energy portion of the absorption spectra.

This scenario also is consistent with the observation that the PL spectrum for the as-trapped NPs looks excitonic. There would always be electrons at the

bottom of the conduction band; therefore whenever a hole is created in the valence band by photoexcitation, emission at the band gap energy can occur. Indeed, one might expect that the PL quantum yield should be quite high. In that case, the low PL intensities for as-trapped QD NPs would require that σ_{abs} must be even smaller than implied by thermal considerations, well below 1% of the solution σ_{abs} for 532 nm excitation.

Nature of the Brightened State. After heating, the emission spectrum is broad, with most of the intensity in three main features peaking near 550 nm, near 650−750 nm, and in the near-IR. The thermally brightened emission is similar for QD monomers, small QD aggregates, and ensembles of QD NPs and also similar for heating by irradiation in the IR or visible. The most easily created damage involves desorption/decomposition of the ligand layer, which creates a variety of surface defect sites.[10−12,46] In the condensed phase, surface sites tend to act as carrier traps, reducing the QY, but also give rise to interband emissive states, some of which are at energies below the band gap. Further evidence suggesting that emission is from surface states was provided by a previous experiment in which a single small QD aggregate was monitored over ∼100 h as it was heated to drive slow sublimation, resulting in ∼80% mass loss.[5] Periodically during the sublimation process, heating was interrupted to allow measurement of emission spectra, which were found to be nearly independent of the mass loss and similar to those observed here and with intensity roughly proportional to the surface area of the NP.

For our Na^+-charged QDs, we cannot rule out the possibility of some charge loss during desorption/decomposition of the ligand layer; however, we know that the final, brightened QD NPs still have 5 to 15 charges. In this final state, without an intact ligand layer isolating the charges from the surface, it may be that a combination of positive charges on the surface and deep surface trap states is able to extract the extra electrons out of the core and trap them, depopulating the conduction band and leading to full or partial reversal of the absorption bleaching. If the conduction band is completely depopulated, then σ_{abs} might be expected to be similar to that for QDs in solution. If that is true, we can use the emission intensity measured for the QD monomers (Figure 5) to estimate the emission QY. For both these examples, the QY is ∼9%, *i.e.*, well below unity, as might be expected for emission from defect states.

Rowland and Shaller[10] reported a study that provides an interesting point of comparison for these results. They deposited octadecylamine-capped CdSe and CdSe/ZnS QDs on glass slides and then annealed them to various temperatures in a vacuum oven, examining the room-temperature PL between each annealing step. For the CdSe QDs, irreversible changes (red shift and loss of PL intensity) were observed at 400 K, *i.e.*, in the range where ligand loss/decomposition is expected to become significant. For CdSe/ZnS QDs, however, irreversible loss of PL was not seen below ∼700 K, which is well above the temperature where the ligand layer would have desorbed/decomposed. Their result shows that the ZnS shell effectively isolated the CdSe core from the effects of changes to the ZnS surface. The situation is clearly different in our experiment, however, because our QD NPs initially have extremely low PL intensity, due to bleaching of σ_{abs} due to electrons populating states near the conduction band minimum. After heating, the emission increases substantially due to the increase in σ_{abs}, but the QY is still well below unity.

CONCLUSION

The PL dynamics of charged QDs in the gas phase is complex, but by taking both the emission behavior and the thermal considerations into account, we have been able to deduce the following:

1. From thermal considerations, it is clear that σ_{abs} must be no more than ∼10% of the solution phase σ_{abs} in order for the QD NPs not to heat to the point of damage.
2. The emission in the unheated state is excitonic, and if our explanation for the weakness of the emission (bleaching of the absorption) is correct, then the emission QY should be near unity, because there are excess electrons in the conduction band available to fill the valence band hole.
3. If the assumption of near-unity QY is correct, then this implies that σ_{abs} for the unheated QD NPs is, in fact, less than 1% of the solution σ_{abs}.
4. The emission after brightening is not excitonic and includes states with energies both higher and lower than the band gap, suggesting that heating creates a wide variety of defect states, such as surface states, which have nonzero emission QY. Some of these emitting states have energies much smaller than the band gap energy.
5. The much brighter emission after heating suggests that the population of extra conduction band electrons, which bleached σ_{abs} for the unheated NPs, is trapped by lower energy surface states, depopulating the conduction band and reversing the bleaching of σ_{abs}.
6. If we assume that σ_{abs} after heating is equal to the solution phase σ_{abs}, we can estimate that the total QY for emission from the diverse range of emitting states ranges from 0.5% to 9%, depending on QD size and excitation wavelength.

Our ultimate interest in QD NPs in the gas phase is for use as noncontact probe particles, allowing us to indirectly track the mass of a nonemitting particle cotrapped with the probe. The QD NPs appear to be

excellent prospects for this purpose, because they have reasonably bright, nonblinking, nonbleaching emission that is stable for days of continuous monitoring,[5] provided only that the visible laser intensity be low enough to prevent sublimation. In addition, however, the gas phase experiments provide a unique perspective on the effects of charge and heating on the photophysics of QDs.

EXPERIMENTAL METHODOLOGY

The experiments were done using an instrument described in detail elsewhere,[13] and only a brief summary is given here. CdSe/ZnS core/shell QDs of various sizes were obtained from NN Laboratories as aqueous solutions and diluted 100:1 in methanol for introduction into the vacuum system by ESI using a commercial z-spray source (Micromass), with a capillary bias of +3.5 kV and cone voltages adjusted to optimize the transmission of NPs in the mass range of interest.

The QD NPs entered the vacuum system as a beam directed into a hexapole ion guide, which guided the NPs through a differential pumping chamber. The NPs then passed through an isolation valve built into an ion lens, into a linear quadrupole ion guide, which acted as a prefilter, selectively transmitting species in the M/Q range of interest. The pneumatically operated isolation valve was used both to gate the NP beam and also to isolate the trap vacuum system from the high flux of air and solvent molecules from the ESI source. After the linear quadrupole, NPs were injected into a split ring-electrode quadrupole trap (SRET), constructed based on a design by Gerlich and coworkers.[1] For efficient trapping the trap region was filled with 10 to 20 mTorr of argon buffer gas.

Positively charged NPs injected into the trap lose energy by collisions with argon and have some probability of being trapped. With experience, it is possible to inject single NPs with reasonably good control, but it is also possible to inject a small ensemble of NPs and then selectively reduce the ensemble to a single NP. Because of aggregation, either in the QD solution used for ESI or in the ESI process itself, it is possible to examine small aggregates ($N < 10$ QDs), in addition to QD monomers. Once trapped, NPs are detected optically using either a continuous wave (cw) 532 nm laser (500 mW maximum power, Ultralasers) or a cw 445 nm laser (2 W maximum). The laser is focused through the trap, passing radially between the two halves of the split-ring electrode. For the experiments described here, we wished to avoid heating the NPs with the PL lasers; therefore a loose focus was used. The beam waist diameter was estimated by moving the laser beam vertically through the trap when a single, large polystyrene particle (~100 nm) was trapped. By measuring the light scattering intensity as a function of position, we determined the beam waists to be ~500 and ~550 μm respectively for the 532 and 445 nm lasers. The trap design also includes a pair of confocal off-axis parabolic mirrors that allow a quasi-cw CO_2 laser (Synrad, 10 W maximum average power) to be focused radially through the trap center for NP heating.

Fluorescence signal was detected at 90° with respect to the laser direction, by collecting light from the trap center through the gap in the split-ring electrode and collimating it with a 25 mm focal length aspheric lens. The collimated light was passed through either a 532 nm notch filter or a 495 nm longpass color filter, to block scattered laser light and optionally passed through additional long-pass color filters and then focused either onto the image plane of an inexpensive CCD camera (Imaging Source) or onto an APD (Laser Components: count 50). From the image magnification and APD size, we estimate that light is collected from a ~50 μm × ~50 μm × 500 μm volume, which we will refer to as the detection volume. The detection solid angle is ~0.34 steradian, limited by the trap electrodes, and taking reflection losses (25−30%) into account, we estimate that the net PL detection efficiency is ~1.5% for wavelengths near the peak of the APD detection efficiency (85% at 670 nm). The other issue that affects detection efficiency is the overlap of the detection volume with the NP ensemble, or the volume of thermal motion in the case of single NPs. For NPs with M and Q in the ranges of interest here, the thermal motion has root-mean-square radial amplitude ranging from ~20 to ~50 μm, with axial amplitude half the radial value.

As discussed by Schlemmer and Gerlich,[1,47] the motion of charged NPs in a quadrupole trap with applied potential at angular frequency Ω and amplitude V_0 can be described at a superposition of fast small amplitude driven motion at Ω, with slow, larger amplitude secular motion with frequency ω_z for motion in the axial direction and ω_r for radial motion. In our setup, we detect the axial motion *via* its effect on the PL collection efficiency. The M/Q for the trapped NP is related to ω_z *via*

$$\frac{M}{Q} = \frac{\sqrt{2}V_0}{\omega_z F z_0^2} \quad (1)$$

where V_0 and Ω are the amplitude and angular frequency of the potential applied to the trap, and z_0 (2.96 mm) is a parameter describing the trap field radius. Unless otherwise stated, for the experiments here, $F = \Omega/2\pi = 143.3$ kHz and $V_0 = 500$ V.

We have developed several approaches to measuring ω_z, depending on the requirements of the experiment with regard to measurement precision and speed. The measurements here primarily focus on the optical properties of trapped QDs, and only modest M/Q precision is required. Therefore, ω_z was measured by applying a low-amplitude (70 mV) sinusoidal drive voltage to one of the trap end-caps. The frequency of this drive potential (f_{drive}) was swept, typically at 0.5 kHz/s, over the frequency range where f_z (= $\omega_z/2\pi$) was expected. When f_{drive} was resonant with f_z, the amplitude of the secular motion increased enough to reduce the time-averaged overlap of the NP position with the PL detection volume. Because the motion was damped by the argon buffer gas, the response appeared as a dip in PL signal at f_z, as illustrated by a typical sweep shown in Figure S2 of the Supporting Information. With the loose focus used here, the detection volume (~50 μm on a side) was mostly determined by the PL collection optics and APD size (100 μm × 100 μm). The speed and precision of the method can be varied by changing the f_{drive} amplitude and sweep rate and the pressure of the argon used to damp the motion. The conditions used here typically gave an M/Q precision of ~0.2% in a measurement taking 30 s. In addition to measuring the secular frequency, the drive voltage can be used to selectively eject NPs from the trap by sweeping over their f_z resonances with high enough drive amplitude. This approach is used below to demonstrate the relationship between the emission spectrum of an ensemble of NPs and the spectra of the individual QD NPs making up the ensemble.

Because this M/Q measurement method is nondestructive, M/Q can be monitored as the NPs are heated, reacted, *etc.*,[5] but for the present purpose the important point is that by monitoring the quantized steps in M/Q (*i.e.*, in ω_z) as a NP undergoes charge-changing collisions with electrons, Ar^+, or Ar* metastables in the chamber background, it is possible to determine the absolute charge and therefore the absolute mass of the NP. A typical example is shown in Figure S2 of the Supporting Information. In the present experiments, a cold cathode vacuum gauge was used to stimulate charge steps. This approach can also be applied to small ensembles of a few trapped NPs, provided that the charge states are low enough that coulomb coupling is weak; however, as more NPs are added, the secular frequency spectrum quickly becomes too congested to interpret reliably.

Emission Spectra. Because the experiments described below were done at low pump laser intensity in order to minimize heating of the NPs, the emission was quite weak; however, at low laser power the emission is stable on a >1 h time scale.

Therefore, to obtain spectral information, we used a series of long-pass color filters. A six-position filter wheel was inserted in the optical path, populated with five filters with cutoff wavelengths of 590, 645, 695, 780, and 850 nm, leaving the sixth position empty for collection of emission filtered only by either a 532 nm notch filter or 495 nm long pass filter, used to block scattered laser light from pump lasers at 532 or 445 nm, respectively. To collect an emission spectrum, signal was counted for 100 s for each color filter. To allow subtraction of background (APD dark counts, scattered laser light), the same procedure was used either immediately before or after the spectral measurement, but with the trap empty of NPs. Under these conditions the reproducibility of the spectra is quite good (<5%), as shown in Figure S1 of the Supporting Information. One issue for these measurements is that if the pump laser intensity is too high, it can heat the NPs enough to change their emission properties. To check whether this had happened during the spectral measurements, the unfiltered signal level was measured before and after each spectral measurement, and if the intensity had changed by more than 5%, the result was discarded.

The emission spectra were obtained by a subtraction process. The raw intensities for each filter wheel position were first corrected using the background spectrum obtained with the trap empty. Next, the signal obtained with the 590 nm cutoff filter was subtracted from the intensity obtained with no color filter, the result being the intensity in the spectral range between 590 nm and either the 532 nm pump laser or the 495 nm cutoff filter used when pumping at 445 nm. The process was repeated for each pair of color filters in order to obtain intensities in the spectral range between their cutoff wavelengths. Finally, the intensity measured with the 850 nm filter inserted represents the intensity between 850 nm and the ~1000 nm sensitivity limit of our APD. The raw spectral intensities were then scaled using information from the APD manufacturer regarding the variation of quantum efficiency with wavelength.

For the purpose of comparison, solution phase emission spectra were measured using the same procedure and pump laser intensities, but replacing the trap with a cuvette containing solutions of the QDs prepared by diluting the commercial stock solution 1:100 in methanol.

This approach to emission spectroscopy gives poor spectral resolution compared to a spectrometer, but its high detection efficiency allows spectra to be acquired at signal levels as low as ~50 counts/s. In principle, it would be possible to generate spectra at lower signal levels by using longer integration times; however, the trade-off is that the QDs are more likely to undergo processes (heating or reactions with background gas) that change their spectral properties during the measurement.

Conflict of Interest: The authors declare no competing financial interest.

Acknowledgment. We would like to thank M. Bartl, P. Guyot-Sionnest, and E. Rabani for helpful discussions. This work was funded by the National Science Foundation, grant number CHE-1111935.

Supporting Information Available: Additional figures, including spectra reproducibility (S1) and an example of the mass and charge determination method (S2) are given. This material is available free of charge *via* the Internet at http://pubs.acs.org.

REFERENCES AND NOTES

1. Schlemmer, S.; Illemann, J.; Wellert, S.; Gerlich, D. Nondestructive High-Resolution and Absolute Mass Determination of Single Charged Particles in a Three-Dimensional Quadrupole Trap. *J. Appl. Phys.* **2001**, *90*, 5410–5418.
2. Trevitt, A. J.; Wearne, P. J.; Bieske, E. J. Calibration of a Quadrupole Ion Trap for Particle Mass Spectrometry. *Int. J. Mass Spectrom.* **2007**, *262*, 241–246.
3. Peng, W. P.; Cai, Y.; Lee, Y. T.; Chang, H. C. Laser-Induced Fluorescence/Ion Trap as a Detector for Mass Spectrometric Analysis of Nanoparticles. *Int. J. Mass Spectrom.* **2003**, *229*, 67–76.
4. Cai, Y.; Peng, W. P.; Chang, H. C. Ion Trap Mass Spectrometry of Fluorescently Labeled Nanoparticles. *Anal. Chem.* **2003**, *75*, 1805–1811.
5. Bell, D. M.; Howder, C. R.; Johnson, R. C.; Anderson, S. L. Single CdSe/Zns Nanocrystals in an Ion Trap: Charge and Mass Determination and Photophysics Evolution with Changing Mass, Charge, and Temperature. *ACS Nano* **2014**, *8*, 2387–2398.
6. Lesnyak, V.; Gaponik, N.; Eychmuller, A. Colloidal Semiconductor Nanocrystals: The Aqueous Approach. *Chem. Soc. Rev.* **2013**, *42*, 2905–2929.
7. Smith, A. M.; Nie, S. Semiconductor Nanocrystals: Structure, Properties, and Band Gap Engineering. *Acc. Chem. Res.* **2010**, *43*, 190–200.
8. Nirmal, M.; Brus, L. Luminescence Photophysics in Semiconductor Nanocrystals. *Acc. Chem. Res.* **1999**, *32*, 407–414.
9. Xiong, W.; Hickstein, D. D.; Schnitzenbaumer, K. J.; Ellis, J. L.; Palm, B. B.; Keister, K. E.; Ding, C.; Miaja-Avila, L.; Dukovic, G.; Jimenez, J. L.; Murnane, M. M.; Kapteyn, H. C. Photoelectron Spectroscopy of CdSe Nanocrystals in the Gas Phase: A Direct Measure of the Evanescent Electron Wave Function of Quantum Dots. *Nano Lett.* **2013**, *13*, 2924–2930.
10. Rowland, C. E.; Schaller, R. D. Exciton Fate in Semiconductor Nanocrystals at Elevated Temperatures: Hole Trapping Outcompetes Exciton Deactivation. *J. Phys. Chem. C* **2013**, *117*, 17337–17343.
11. Zhao, Y.; Riemersma, C.; Pietra, F.; Koole, R.; Donegá, C. d. M.; Meijerink, A. High-Temperature Luminescence Quenching of Colloidal Quantum Dots. *ACS Nano* **2012**, *6*, 9058–9067.
12. Bullen, C.; Mulvaney, P. The Effects of Chemisorption on the Luminescence of CdSe Quantum Dots. *Langmuir* **2006**, *22*, 3007–3013.
13. Howder, C. R.; Bell, D. M.; Anderson, S. L. Optically Detected, Single Nanoparticle Mass Spectrometer with Prefiltered Electrospray Nanoparticle Source. *Rev. Sci. Instrum.* **2014**, *85*, 014104–014110.
14. Guyot-Sionnest, P. Charging Colloidial Quantum Dots by Electrochemistry. *Microchim. Acta* **2008**, *160*, 309–314.
15. Galland, C.; Ghosh, Y.; Steinbruck, A.; Sykora, M.; Hollingsworth, J. A.; Klimov, V. I.; Htoon, H. Two Types of Luminescence Blinking Revealed by Spectroelectrochemistry of Single Quantum Dots. *Nature* **2011**, *479*, 203–208.
16. Rinehart, J. D.; Schimpf, A. M.; Weaver, A. L.; Cohn, A. W.; Gamelin, D. R. Photochemical Electronic Doping of Colloidal CdSe Nanocrystals. *J. Am. Chem. Soc.* **2013**, *135*, 18782–18785.
17. Mocatta, D.; Cohen, G.; Schattner, J.; Millo, O.; Rabani, E.; Banin, U. Heavily Doped Semiconductor Nanocrystal Quantum Dots. *Science* **2011**, *332*, 77–81.
18. Shim, M.; Wang, C.; Norris, D. J.; Guyot-Sionnest, P. Doping and Charging in Colloidal Semiconductor Nanocrystals. *MRS Bull.* **2001**, *26*, 1005–1008.
19. Gupta, S.; Kershaw, S. V.; Rogach, A. L. 25th Anniversary Article: Ion Exchange in Colloidal Nanocrystals. *Adv. Mater.* **2013**, *25*, 6923–6944.
20. Yalcin, S. E.; Labastide, J. A.; Sowle, D. L.; Barnes, A. M. D. Spectral Properties of Multiply Charged Semiconductor Quantum Dots. *Nano Lett.* **2011**, *11*, 4425–4430.
21. Kittel, C. *Introduction to Solid State Physics*; John Wiley: New York, 1986.
22. Zinc Sulfide, Ipcs International Programme on Chemical Safety. http://www.inchem.org/documents/icsc/icsc/eics1627.htm.
23. Cadmium Selenide (CdSe) Debye Temperature, Heat Capacity, Density, Melting Point, Hardness. In *II-VI and I-VII Compounds; Semimagnetic Compounds*; Madelung, O.; Rössler, U.; Schulz, M., Eds.; Springer: Berlin, 1999; Vol. 41B, pp 1–3.
24. Goris, B.; Van Huis, M. A.; Bals, S.; Zandbergen, H. W.; Manna, L.; Van Tendeloo, G. Thermally Induced Structural and Morphological Changes of CdSe/CdS Octapods. *Small* **2012**, *8*, 937–942.
25. van de Hulsst, H. C. *Light Scattering by Small Particles*; Dover: New York, 1981.

26. Bohren, C. F.; Huffman, D. R. *Absorption and Scattering of Light by Small Particles*; Wiley: New York, 1983.
27. Landstrom, L.; Elihn, K.; Boman, M.; Granqvist, C. G.; Heszler, P. Analysis of Thermal Radiation from Laser-Heated Nanoparticles Formed by Laser-Induced Decomposition of Ferrocene. *Appl. Phys. A: Mater. Sci. Process.* **2005**, *81*, 827–833.
28. Landstrom, L.; Heszler, P. Analysis of Blackbody-like Radiation from Laser-Heated Gas-Phase Tungsten Nanoparticles. *J. Phys. Chem. B* **2004**, *108*, 6216–6221.
29. Roura, P.; Costa, J. Radiative Thermal Emission from Silicon Nanoparticles: A Reversed Story from Quantum to Classical Theory. *Eur. J. Phys.* **2002**, *23*, 191–203.
30. Yu, W. W.; Qu, L.; Guo, W.; Peng, X. Experimental Determination of the Extinction Coefficient of CdTe, CdSe, and CdS Nanocrystals. *Chem. Mater.* **2003**, *15*, 2854–2860.
31. Jasieniak, J.; Smith, L.; Embden, J. v.; Mulvaney, P.; Califano, M. Re-examination of the Size-Dependent Absorption Properties of CdSe Quantum Dots. *J. Phys. Chem. C* **2009**, *113*, 19468–19474.
32. Sun, J.; Goldys, E. M. Linear Absorption and Molar Extinction Coefficients in Direct Semiconductor Quantum Dots. *J. Phys. Chem. C* **2008**, *112*, 9261–9266.
33. Leatherdale, C. A.; Woo, W.-K.; Mikulec, F. V.; Bawendi, M. G. On the Absorption Cross Section of CdSe Nanocrystal Quantum Dots. *J. Phys. Chem. B* **2002**, *106*, 7619–7622.
34. Cadmium Selenide (CdSe) Thermodynamical Properties, Phase Diagram. In *II-VI and I-VII Compounds; Semimagnetic Compounds*, Madelung, O.; Rössler, U.; Schulz, M., Eds.; Springer: Berlin, 1999; Vol. 41B, pp 1−7.
35. Watt, W.; Moreton, R.; Carpenter, L. G. The Thermal Accommodation of Helium and Argon on a Tungsten Wire, Deduced from the Heat Lost by the Wire. *Surf. Sci.* **1974**, *45*, 238–248.
36. Grimmelmann, E. K.; Tully, J. C.; Cardillo, M. J. Hard-Cube Model Analysis of Gas-Surface Energy Accommodation. *J. Chem. Phys.* **1980**, *72*, 1039–1043.
37. King, M. E.; Nathanson, G. M.; Hanning-Lee, M. A.; Minton, T. K. Probing the Microscopic Corrugation of Liquid Surfaces with Gas-Liquid Collisions. *Phys. Rev. Lett.* **1993**, *70*, 1026–1029.
38. Alexander, W. A.; Zhang, J.; Murray, V. J.; Nathanson, G. M.; Minton, T. K. Kinematics and Dynamics of Atomic-Beam Scattering on Liquid and Self-Assembled Monolayer Surfaces. *Faraday Discuss.* **2012**, *157*, 355–374.
39. Pong, B.-K.; Trout, B. L.; Lee, J.-Y. Modified Ligand-Exchange for Efficient Solubilization of CdSe/ZnS Quantum Dots in Water: A Procedure Guided by Computational Studies. *Langmuir* **2008**, *24*, 5270–5276.
40. Lavrich, D. J.; Wetterer, S. M.; Bernasek, S. L.; Scoles, G. Physisorption and Chemisorption of Alkanethiols and Alkyl Sulfides on Au(111). *J. Phys. Chem. B* **1998**, *102*, 3456–3465.
41. Kang, H.; Kim, Y.; Park, T.; Park, J. B.; Ito, E.; Hara, M.; Noh, J. Surface Structures and Thermal Desorption Behaviors of Cyclopentanethiol Self-Assembled Monolayers on Au(111). *Bull. Korean Chem. Soc.* **2011**, *32*, 1253–1257.
42. Zhang, Y.; Schnoes, A. M.; Clapp, A. R. Dithiocarbamates as Capping Ligands for Water-Soluble Quantum Dots. *ACS Appl. Mater. Interfaces* **2010**, *2*, 3384–3395.
43. Lias, S. G.; Bartmess, J. E.; Liebman, J. F.; Holmes, J. L.; Levin, R. D.; Mallard, W. G. *Ion Energetics Data*. National Institute of Standards and Technology: Gaithersburg, MD (http://webbook.nist.gov), 2000.
44. Fang, X.; Bando, Y.; Shen, G.; Ye, C.; Gautam, U. K.; Costa, P. M. F. J.; Zhi, C.; Tang, C.; Golberg, D. Ultrafine ZnS Nanobelts as Field Emitters. *Adv. Mater.* **2007**, *19*, 2593–2596.
45. Shim, M.; Wang, C.; Guyot-Sionnest, P. Charge-Tunable Optical Properties in Colloidal Semiconductor Nanocrystals. *J. Phys. Chem. B* **2001**, *105*, 2369–2373.
46. Voznyy, O.; Thon, S. M.; Ip, A. H.; Sargent, E. H. Dynamic Trap Formation and Elimination in Colloidal Quantum Dots. *J. Phys. Chem. Lett.* **2013**, *4*, 987–992.
47. Schlemmer, S.; Illemann, J.; Wellert, S.; Gerlich, D. Non-destructive, Absolute Mass Determination of Submicrometer Sized Particles in a Paul-Type Trap. *AIP Conf. Proc.* **1999**, *457*, 80–86.